



HAL
open science

Dimethomorph degradation in vineyards examined by isomeric and isotopic fractionation

Jérémy Masbou, Sylvain Payraudeau, Benoit Guyot, Gwenaël Imfeld

► **To cite this version:**

Jérémy Masbou, Sylvain Payraudeau, Benoit Guyot, Gwenaël Imfeld. Dimethomorph degradation in vineyards examined by isomeric and isotopic fractionation. *Chemosphere*, 2023, 313, pp.137341. 10.1016/j.chemosphere.2022.137341 . hal-03872967

HAL Id: hal-03872967

<https://hal.science/hal-03872967>

Submitted on 26 Nov 2022

HAL is a multi-disciplinary open access archive for the deposit and dissemination of scientific research documents, whether they are published or not. The documents may come from teaching and research institutions in France or abroad, or from public or private research centers.

L'archive ouverte pluridisciplinaire **HAL**, est destinée au dépôt et à la diffusion de documents scientifiques de niveau recherche, publiés ou non, émanant des établissements d'enseignement et de recherche français ou étrangers, des laboratoires publics ou privés.

1 Dimethomorph degradation in vineyards
2 examined by isomeric and isotopic fractionation

3
4 *Jérémy Masbou¹, Sylvain Payraudeau¹, Benoit Guyot¹, Gwenaël Imfeld^{1,*}*

5
6 ¹Université de Strasbourg, CNRS, ENGEES, ITES UMR7063, F-67084 Strasbourg, France.

7
8 **RECEIVED DATE**

9 * Corresponding author:

10 Gwenaël Imfeld, Ph.D.

11 Université de Strasbourg, CNRS, ENGEES, ITES UMR7063, F-67084 Strasbourg, France.

12 E-mail: imfeld@unistra.fr

13
14
15
16
17
18 Manuscript for Chemosphere

20 **Abstract**

21 Knowledge of the degradation extent and pathways of fungicides in the environment is
22 scarce. Fungicides may have isomers with distinct fungal-control efficiency, toxicity and fate
23 in the environment, requiring specific approaches to follow up the degradation of individual
24 isomers. Here we examined the degradation of the widely used fungicide dimethomorph
25 (DIM) in a vineyard catchment using the signatures of carbon stable isotopes ($\delta^{13}\text{C}$) and E/Z
26 isomer fractionation (IF(Z)). In a microcosm laboratory experiment, DIM degradation half-
27 life in soil was 20 ± 3 days, and was associated with significant isomeric ($\Delta\text{IF}(\text{Z}) = +30\%$)
28 and isotopic ($\Delta\delta^{13}\text{C}$ up to 7 ‰) fractionation. This corresponds to an isomer enrichment factor
29 of $\epsilon_{\text{IR}} = -54 \pm 6\%$, suggesting isomer selectivity and similar carbon stable isotopic
30 fractionation values of $\epsilon_{\text{DIM-(Z)}} = -1.6 \pm 0.2 \text{ ‰}$ and $\epsilon_{\text{DIM-(E)}} = -1.5 \pm 0.2 \text{ ‰}$. Isomeric and
31 isotopic fractionation values were used to estimate DIM degradation in topsoil and transport
32 in a vineyard catchment over two wine-growing seasons. DIM concentrations following DIM
33 application were up to $3 \mu\text{g}\cdot\text{g}^{-1}$ in topsoil and $29 \mu\text{g}\cdot\text{L}^{-1}$ in runoff water at the catchment
34 outlet. Accordingly, the IF(Z) and $\delta^{13}\text{C}$ values of DIM in soil were similar to those observed
35 in DIM commercial formulations. The gradual enrichments in DIM-(Z) and ^{13}C of the
36 residual DIM in soil indicated DIM biodegradation over time. DIM biodegradation estimated
37 based on E/Z isomer and carbon stable isotope ratios in topsoil and runoff water ranged from
38 0% after DIM application up to 100% at the end of the wine-growing season. DIM
39 biodegradation was overestimated compared to conventional approaches relying on DIM
40 mass balance, field concentrations and half-lives. Altogether, our study highlights the
41 usefulness of combining carbon isotopes, E/Z isomers and classical approaches to estimate
42 fungicide degradation at the catchment scale, and uncovers difficulties in using laboratory-
43 derived values in field studies.

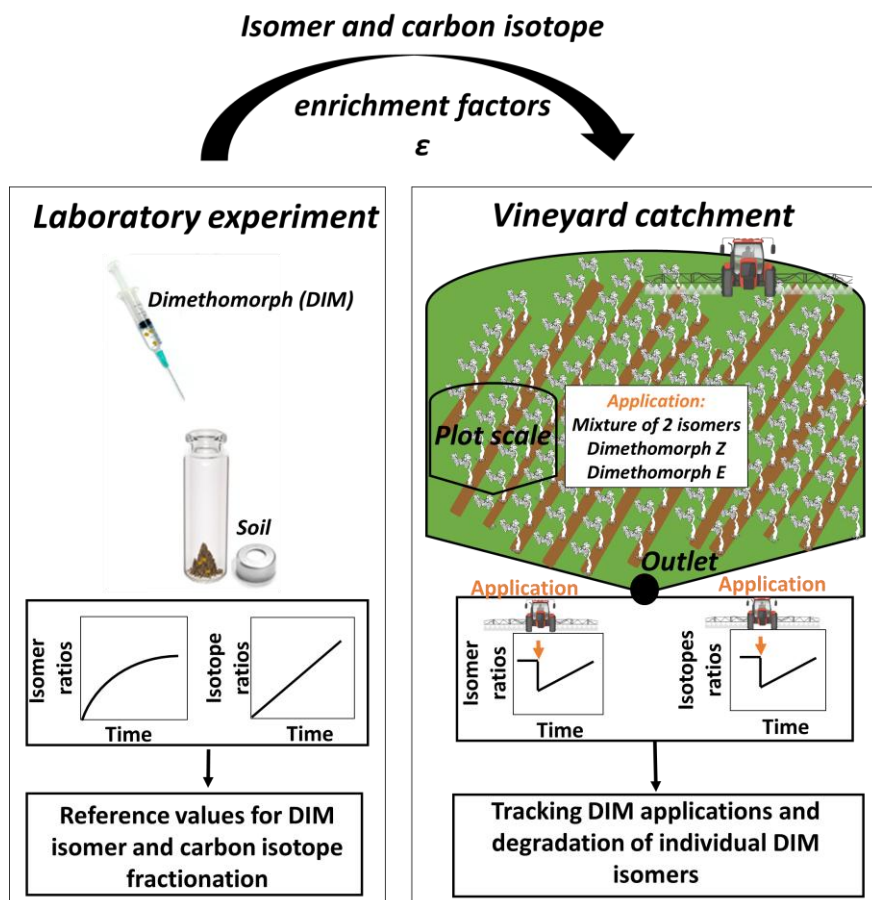
44 KEYWORDS: Dimethomorph, isotopes, isomers, CSIA, ISIA, vineyard, pesticides

45 HIGHLIGHTS:

- 46 • Degradation estimates of dimethomorph (DIM), a widely used fungicide in vineyards
- 47 • DIM half-life of 20 ± 3 days in vineyard topsoil
- 48 • DIM isomer selectivity ($\epsilon_{IR} = -54 \pm 6\%$) during biodegradation
- 49 • Carbon isotopic fractionation (ϵ_c) similar for DIM-(E) and DIM-(Z) biodegradation
- 50 • Stable isotopes and isomers to estimate DIM degradation at the catchment scale

51

52 TOC-ART:



53

54

56 1. Introduction

57 The proportion of modern pesticide formulations with active ingredients containing
58 several isomers has gradually increased over the last decade (Jeschke, 2018). Stereoisomers
59 are molecules with the same molecular formula and constitution, but differing in the three-
60 dimensional orientations of their atoms in space. The great majority of manufactured
61 stereoisomeric pesticides are mixture of stereoisomers, although the bioactivity is primarily
62 associated with only one stereoisomer (Kurihara et al., 1997). Individual stereoisomers,
63 however, may differ in pest-control efficiency (Garrison, 2006), toxicity (Huang et al., 2012;
64 Xie et al., 2018; Zhai et al., 2019), and fate (Buser et al., 2000; Gámiz et al., 2016; Hegeman
65 and Laane, 2002). Within stereoisomers, diastereoisomers (e.g., (E)/(Z)) are molecules which
66 are neither superimposable nor the image of each other in a mirror. In environmental studies,
67 stereochemistry is often neglected, while isomers are considered as a unique molecular entity.
68 Stereoisomer-specific studies are thus crucial to assess the risks associated with
69 stereoisomeric pesticides (Basheer, 2018; de Albuquerque et al., 2018; Liu et al., 2005; Petrie
70 et al., 2015).

71 The widely used fungicide dimethomorph (4-[3-(4-chlorophenyl)-3-(3,4-dimethoxy-
72 yphenyl) acryloyl] morpholine) (DIM) contains a double bond and consists of the
73 stereoisomers DIM-(E) and DIM-(Z). The frequent detection of DIM in vineyard soils, waters
74 and grapes mirrors regular DIM applications and moderate DIM degradation in soil (half-life
75 $T_{1/2}$ range: 41-96 days in aerobic soils (EFSA, 2006)), posing a risk for surrounding living
76 organisms (Imfeld et al., 2020; Liu et al., 2012; Shabeer et al., 2015). DIM was selected in
77 this study as a model stereoisomeric pesticide because (i) it is used worldwide and in several
78 crops to control plant diseases, such as mildew and root rot, (ii) the fungicidal activity stems

79 from the (Z)-isomer of DIM (PPDBwebsite), although commercial formulations are not
80 enriched in the (Z)-isomer, and (iii) knowledge of the degradation of individual DIM
81 stereoisomers and the direction of stereoselective degradation of DIM is scarce.

82 Among degradative and nondegradative processes contributing to pesticide dissipation
83 in the environment, DIM biodegradation may be isomer-selective (Huang et al., 2012; Li et
84 al., 2012; Masbou et al., 2018b). DIM biodegradation with preferential use of the E-
85 stereoisomer has been reported (Jia and Zhu, 2015; Suryawanshi et al., 2018; Zhang et al.,
86 2020), supporting the use of isomeric ratios as a DIM biodegradation proxy. In stereoisomeric
87 pollutants, one isomer may degrade faster than the other due to preferential microbial uptake
88 or enzyme activity, stemming from different geometrical recognitions of the isomer molecules
89 (Jammer et al., 2014). Hence, gradual changes in the isomeric fractions (IF) or ratios (IR)
90 from the initial isomeric signature may help evaluate degradation in the field (Jin and Rolle,
91 2016; Williams et al., 2003). However, this approach may be limited for DIM due to its
92 sensitivity to isomerization mechanisms (i.e., interconversion of (E) and (Z) isomers, (Avetta
93 et al., 2014)) and the isomer-selective dependence of DIM degradation on specific soil
94 properties, such as organic matter and pH (Li et al., 2013; Yang and Ji, 2015).

95 In this context, combining isomer analysis and compound-specific stable isotope
96 analysis (CSIA) in the so-called isomer-selective isotope analysis (ISIA or ESIA for
97 enantiomer-specific cases) may help to identify sources and transformations of pesticide
98 isomers in the environment (Badea and Danet, 2015; Maier et al., 2013). Similar to isomers,
99 pesticide molecules with light and heavy stable isotopes are degraded at slightly different
100 rates, which results in a kinetic isotope effect (Hoefs, 1997). Pesticide CSIA can be used to
101 evaluate the *in situ* biodegradation of pesticides and has been applied in various experimental
102 settings (Cui et al., 2021; Drouin et al., 2021; Droz et al., 2021; Masbou et al., 2018a;
103 Melsbach et al., 2020; Meyer et al., 2009; Pérez-Rodríguez et al., 2021; Torrentó et al., 2021)

104 and in modelling studies (Lutz et al., 2017). However, field studies involving the pesticide
105 CSIA (Alvarez-Zaldívar et al., 2018; Wu et al., 2018) remain limited thus far, mainly due to
106 conceptual and analytical limits. ESIA has been developed for several chiral compounds (e.g.,
107 polar herbicides, HHCB, phenoxyalkanoic methyl herbicides, anilide fungicides and PCBs)
108 (Jammer et al., 2014; Maier et al., 2013; Masbou et al., 2018b; Milosevic et al., 2013; Tang et
109 al., 2017; Wang et al., 2013). In contrast, ISIA is currently limited to hexachlorocyclohexane
110 (HCH) isomers (Badea et al., 2011; Bashir et al., 2013; Zhang et al., 2014). Here we
111 hypothesised that the application of DIM-ISIA may help to evaluate the contribution of DIM
112 biodegradation to the overall DIM dissipation in the field, where both degradative and
113 nondegradative processes co-occur.

114 The purpose of this study was thus to examine the degradation and transport of DIM
115 isomers at the scale of a small (42.7 ha) vineyard catchment (Rouffach, France) using isotopic
116 and isomeric signatures. ISIA and isomeric ratios measurements were developed for DIM
117 isomers and applied to both laboratory microcosm experiments and field samples to evaluate
118 (i) the degradation of DIM isomers in vineyard topsoil and runoff water, and (ii) the
119 applicability of isomeric and isotopic approaches to estimate the contribution of degradation
120 to the overall DIM dissipation at the catchment scale.

121 **2. Materials and methods**

122 *2.1. Chemicals and solution preparation*

123 DIM standard (PESTANAL, purity: >97%), metolachlor-d11 (analytical grade purity,
124 >97%), solvents (dichloromethane DCM, acetonitrile ACN, ethyl acetate EtOAc; HPLC
125 grade purity, >99.9%) and sulfate magnesium (MgSO₄, ReagentPlus® ≥99.5%) were
126 purchased from Sigma–Aldrich. Primary secondary amide (PSA)-bonded silica was

127 purchased from Supelco. For further calibration standard preparation and reproducibility
128 check, a stock solution of DIM at 1 g.L^{-1} was prepared in dichloromethane (DCM) and stored
129 at $-18 \text{ }^{\circ}\text{C}$ until analysis. In the absence of DIM(E) or DIM(Z) standards, all measurements and
130 experiments were carried out using available DIM standard from Sigma-Aldrich ($\text{IF(Z)} = 0.61$
131 ± 0.01 , $n=10$).

132 **2.2. Study site**

133 The 42.7 ha Hohrain vineyard catchment is located in the Alsatian foothills ($47^{\circ}57'9$
134 N, $07^{\circ}17'3$ E) and is representative of northern vineyards (Duplay et al., 2014; Imfeld et al.,
135 2020) (Figure S1). The catchment has a mean slope of 15% and is mainly occupied by
136 vineyards (59%, 25.3 ha), forests and pasture (29%), grass strips and ditches (7%), and roads
137 and paths (5%). The soil is a calcareous clay loam developed on a loess basement with a bulk
138 density of 1.4 g cm^{-3} . The main soil types are Cambisol (Hypereutric Clayic) and Haplic
139 Cambisol (Calcaric Siltic) (Duplay et al., 2014). Vineyard plots are permanently covered by
140 grass every second inter row to limit soil erosion, and grass-free interrows are ploughed down
141 to a 5 cm depth to enhance water infiltration.

142 Rainfall-runoff events generate intermittent discharge at the outlet of the catchment,
143 driven by Hortonian overland flow. Vineyard plots contribute to discharge when rainfall
144 intensity overcomes saturated hydraulic conductivity (Tournebize et al., 2012). Grass strips
145 with a 2 to 3 m width at the plot edges limit overland flow on plots (Lefrancq et al., 2014).

146 **2.3. Pesticide applications and sampling**

147 The dose and frequency of pesticide applications were obtained from surveys
148 addressed to wine producers of the catchment in 2015 and 2016. Answers from producers
149 covered 75% and 74% of the total vineyard area in 2015 and 2016, respectively. The dose and
150 timing of applications were extrapolated for the non-surveyed area to calculate the seasonal

151 pesticide applications. The amount of DIM applications in the vineyard catchment estimated
152 by surveys of the farmers was 119 g in 2015 and 5406 g in 2016 (Dose: 2 to 6 kg.ha⁻¹) (Imfeld
153 et al., 2020). The high mildew pressure in 2016 associated with unfavourable wet and warm
154 climatic conditions in early summer explained the significant difference in applied amounts
155 between the two years. DIM was applied on June 19th in 2015 and between June 20th and 23rd
156 in 2016.

157 The sampling procedure is detailed in Table S1. Briefly, topsoil samples (0-1 cm)
158 were collected weekly from March to October 2015 and 2016 across four transects across the
159 catchment (Figure S1) (Imfeld et al., 2020). Topsoil samples were also collected every 7 to 30
160 days in two adjacent and representative vineyard plots, 1486 m² each, namely, P1 and P2
161 (locations on Figure S1). Composite topsoil samples (1 kg) consisted of mixed topsoil
162 subsamples collected every 10 m across the transects in the catchment and every 2 m across 5
163 interrows for each plot. Topsoil samples were transported in coolers and stored at -18 °C until
164 DIM extraction.

165 Runoff samples were collected at the catchment and plot outlets (Imfeld et al., 2020).
166 Briefly, automatic runoff measurement and water sampling were carried out from March 26th
167 to October 6th, 2015, and from March 30th to October 10th, 2016. Water depth was measured
168 at the catchment outlet using a bubbler flow module (Hydrologic) combined with a Venturi
169 channel to monitor discharge runoff, with an uncertainty of ±8%. Flow proportional samples
170 (100 ml every 6 L) of runoff water were collected during each runoff event using a 4010
171 Hydrologic automatic refrigerated sampler. Runoff water was collected in a 24-bottle sampler
172 with precleaned glass bottles.

173 Runoff water from the plots was collected in a gutter located downstream of each plot.
174 The gutters were covered to limit photolysis and contamination during the passage of
175 agricultural machinery. Water flow at the outlet of the plots was monitored continuously

176 using an ultrasonic height sensor (ISMA) connected to a flowmeter and combined with an
177 exponential section Venturi channel (ISMA). Runoff water samples were collected in
178 proportion to the flow rate at each flowing event (100 mL every 3 L) using a flow-controlled
179 refrigerated automatic sampler (ISCO). Samples were combined weekly into a composite
180 sample. Water samples were refrigerated during sampling and placed on ice during transport
181 to the laboratory to limit pesticide degradation. Water samples were immediately filtered
182 using a 0.45 μm glass filter membrane and frozen ($-18\text{ }^{\circ}\text{C}$) until extraction and DIM analysis.

183 ***2.4. DIM biodegradation experiment in microcosms***

184 Topsoil (0-5 cm) from the vineyard plots (Table S3 for soil physicochemical
185 characteristics) was collected and pooled on August 6th, 2015, to evaluate isomer and isotope
186 fractionation during aerobic DIM biodegradation. The DIM concentration in topsoil before
187 DIM spiking was below the LOD. The soil microcosms consisted of 30 mL glass vials. To
188 maintain aerobic conditions while limiting water loss and avoiding contamination, a 0.2 μm
189 syringe filter (Rotilabo®, Carl Roth®, France) was mounted on a syringe tip stuck through
190 the vial cap (see experimental setup in the SI, Figure S5). Approximately 15 g of soil was
191 incubated, and deionized water was added to reach a volumetric water content of 20% of soil.
192 The soil was spiked with an environmentally relevant concentration of 10 $\mu\text{g}\cdot\text{g}^{-1}$ DIM. Abiotic
193 control experiments were prepared similarly to sterilized soils (autoclaved three times at 12-
194 hour intervals). Ten separate experiments and 10 abiotic controls were incubated at $20 \pm 1\text{ }^{\circ}\text{C}$
195 and collected using a sacrificial approach at Days 1, 10, 25, 50 and 100 (duplicate
196 measurements at each sampling date).

197 ***2.5. Dimethomorph extraction and analysis***

198 DIM was extracted from water samples using solid-phase extraction (SPE) and from
199 soil samples using QUECHERS modified extraction procedures, as previously described

200 (Gilevska et al., 2022). DIM isomers were quantified by gas chromatography (Trace 1300,
 201 Thermo Fisher Scientific) coupled with a mass spectrometer (ISQTM, Thermo Fisher
 202 Scientific) using a Metolachlor-d11 isotope-labelled internal standard. As the DIM standard
 203 was not certified in DIM(E) and DIM(Z) isomers, the ratios of peak areas for DIM(E) and
 204 DIM(Z) isomers obtained from GC-MS in SIM/Fullscan mode and GC-IRMS were used to
 205 characterize the DIM standard. Both GC-MS and GC-IRMS measurements gave similar and
 206 reproducible ($IF(Z) = 0.61 \pm 0.1$) isomer ratios. Distinct calibrations curves were then
 207 obtained to evaluate separately DIM(E) and DIM(Z) concentrations. Extraction recoveries,
 208 DL and QL from water and soil samples are provided in Table S2.

209 DIM isomer separation was sufficient for accurate isotope analysis (isomer resolution,
 210 $R > 2$) (Hengel and Shibamoto, 2000). Typical chromatograms (pure standard, water and
 211 topsoil samples) are provided in SI (Figure S2). The soil extraction procedure had no
 212 significant effect on the Z/E isomer ratios and the carbon isotope composition (SI, Section S-
 213 3).

214 **2.6. Carbon stable isotope analysis of dimethomorph**

215 The carbon isotope compositions of DIM isomers ($\delta^{13}C_{DIM-(Z)}$ and $\delta^{13}C_{DIM-(E)}$) were
 216 determined using a GC-C-IRMS system consisting of a gas chromatograph (Trace GC Ultra,
 217 Thermo Fisher Scientific) coupled *via* a GC IsoLink/Conflo IV interface (Thermo Fisher
 218 Scientific) to an isotope ratio mass spectrometer (DeltaV Plus, Thermo Fisher Scientific). The
 219 $\delta^{13}C$ values were calibrated using a three-point calibration using the international reference
 220 materials AIEA-600, USGS-40, and USGS-41 ($\sigma < 0.05$ ‰) and reported in parts per thousand
 221 (‰) against the Vienna Pee Dee Belemnite (VPDB) reference standard, according to Equation
 222 1:

$$223 \quad \delta^{13}C_{DIM-(X)} = \left(\frac{(^{13}C_{DIM-(X)}/^{12}C_{DIM-(X)})_{sample}}{(^{13}C_{CO_2}/^{12}C_{CO_2})_{ref}} - 1 \right) \times 1000 \quad (1)$$

224 with $X = \text{bulk, (Z) or (E)}$

225 Details of the DIM-ISIA validation protocol are provided in the SI (Section S-3).
226 Briefly, linearity tests were performed on DIM standards, indicating a minimum injection of 6
227 ngC for both DIM-(E) and DIM-(Z) for reliable DIM CSIA. The measurement precision of
228 $\delta^{13}\text{C}_{\text{DIM-(Z)}} = -33.6 \pm 0.7 \text{‰}$ ($\pm \sigma$, $n = 20$) was similar to that of $\delta^{13}\text{C}_{\text{DIM-(E)}} = -33.5 \pm 0.7 \text{‰}$ and
229 $\delta^{13}\text{C}_{\text{Bulk-DIM}} = -33.5 \pm 0.5 \text{‰}$. The total analytical uncertainty of $\sigma < 0.7 \text{‰}$ for amplitude >100
230 mV (m/z 44) on each isomer (>6 ngC) was consistent with typical CSIA measurements
231 (Schürner et al., 2016). Long-term $\delta^{13}\text{C}$ values obtained during 3 different GC-C-IRMS
232 sessions within 3 months (Figure S4 and Table S2) did not significantly differ from the bulk
233 value ($\delta^{13}\text{C}_{\text{Bulk-DIM}} = -33.0 \pm 0.5 \text{‰}$; $\pm \sigma$, $n = 3$) obtained with an elemental analyser-isotopic
234 ratio mass spectrometer (Flash EA IsoLink™ CN IRMS, Thermo Fisher Scientific). Cross-
235 calibration of the DIM Sigma–Aldrich standard confirmed insignificant isotopic fractionation
236 associated with the extraction procedure and DIM-ISIA.

237 Despite the robustness of DIM-ISIA analytical method, several field samples ($n = 50$)
238 failed the quality check due to either low concentrations, yielding peak amplitude <100 mV,
239 or co-elution. The validated DIM-ISIA measurements ($n = 29$) were thus limited, leading to a
240 discrepancy between soil and water samples in 2015 and 2016.

241 ***2.7. Isomeric fractionation and carbon isotope calculations***

242 Change in the proportion of each isomer was calculated by isomer fractionation IR(Z)
243 and IF(Z) isomeric ratio and fractionation respectively, and according to:

$$244 \quad \text{IR(Z)} = \frac{[\text{DIM-(Z)}]}{[\text{DIM-(E)}]} \quad (2)$$

$$245 \quad \text{IF(Z)} = \frac{[\text{DIM-(Z)}]}{[\text{DIM-(Z)}] + [\text{DIM-(E)}]} \quad (3)$$

246 *Rac*-DIM mixture thus displays $\text{IR(Z)} = 1$ and $\text{IF(Z)} = 0.5$, while an enrichment in
247 DIM-(Z) features an $\text{IR(Z)} > 1$ and $\text{IF(Z)} > 0.5$.

248 An isotopic balance calculation enabled determining the isotopic composition of
 249 bulk-DIM ($\delta^{13}\text{C}_{\text{bulk-DIM}}$) from the stable isotope ratios of the individual DIM isomers
 250 determined by GC-C-IRMS (Badea et al., 2011):

$$251 \quad \delta^{13}\text{C}_{\text{Bulk-DIM}} = IF_{\text{DIM-(Z)}} \times \delta^{13}\text{C}_{\text{DIM-(Z)}} + IF_{\text{DIM-(E)}} \times \delta^{13}\text{C}_{\text{DIM-(E)}} \quad (4)$$

252 The bulk-DIM $\delta^{13}\text{C}_{\text{bulk-DIM}}$ of the analytical standard was also determined by GC-
 253 IRMS analysis as a double-peak integration method and by EA-IRMS, confirming the
 254 isotopic balance approach (Table S2). Isotopic fractionation values (ϵ) for DIM-(E) and DIM-
 255 (Z) were calculated from the logarithmic linearization using the Rayleigh equation:

$$256 \quad \ln\left(\frac{\delta^{13}\text{C}_x+1}{\delta^{13}\text{C}_0+1}\right) = \epsilon \times \ln\left(\frac{C_x}{C_0}\right) \quad (5)$$

257 where $\delta^{13}\text{C}_0$ and $\delta^{13}\text{C}_x$ are the measured carbon isotope ratios at the beginning ($t = 1$ day) and
 258 at $t = x$ days from the beginning of the experiment, and C_0 and C_x are the corresponding
 259 concentrations.

260 The carbon isotopic fractionation value (ϵ), derived from closed soil degradation experiments
 261 under mixed aerobic conditions, were used to quantify field degradation B(%) (Alvarez-
 262 Zaldívar et al., 2018; Höhener et al., 2022; Hunkeler et al., 2008):

$$263 \quad B(t, \%) = \left(1 - \left(\frac{\delta^{13}\text{C}_t + 1000}{\delta^{13}\text{C}_0 + 1000}\right)^{\frac{1000}{\epsilon}}\right) \times 100 \quad (6)$$

264 Similarly, the Rayleigh equation allows deriving isomeric enrichment factors ϵ_{IR} from linear
 265 regression of:

$$266 \quad \ln\left(\frac{IR(Z)x}{IR(Z)0}\right) = \epsilon_{\text{IR}} \times \ln\left(\frac{C_x}{C_0}\right) \quad (7)$$

267 IR is generally preferred to IF for ϵ_{IR} calculations (Jammer et al., 2014). The carbon isotopic
268 fractionation value (ϵ_{IR}), derived from closed soil degradation experiments under mixed
269 aerobic conditions, were used to quantify field degradation B(%):

$$270 \quad B(t, \%) = \left(1 - \left(\frac{\text{IR}(Z)_t}{\text{IR}(Z)_0}\right)^{\frac{1}{\epsilon}}\right) \times 100 \quad (8)$$

271 The error of the isotopic fractionation values and the isomeric enrichment factors was given
272 as the 95% confidence interval (CI) and determined using regression analysis, as described
273 elsewhere (Elsner et al., 2007).

274 **2.9. Statistical analysis**

275 Statistical analyses were carried out using JMP software (SAS Institute, USA) and the
276 function “Data Analysis” from the Add-In “Analysis Tool Pack” of Microsoft Excel®.
277 Isotopic and isomeric fractionation values were calculated from linear regressions of Equation
278 (5) and (7) respectively, and rate constants (or half-lives) were determined using a single first-
279 order rate model (SFO) from plots of $\ln(C/C_0)$ versus time (see SI for details). Measurements
280 were performed in triplicate and all data are displayed as the mean \pm 95% CI unless otherwise
281 specified.

282 **3. Results and discussion**

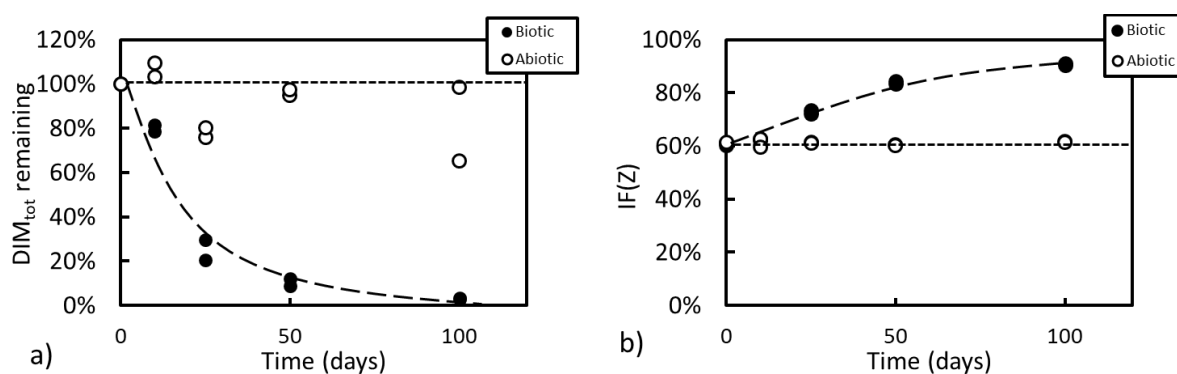
283 **3.1. Isomer-selective biodegradation of DIM in soil microcosms**

284 In abiotic microcosm experiments, DIM_{tot} concentrations in soils did not vary over
285 time (Figure 1), except on Day 100 ($[\text{DIM}]_{t=100}/[\text{DIM}]_{t=1} = 0.65$) in a single replicate. High
286 DIM half-lives ($T_{1/2} > 100$ days) in abiotic experiments coincided with insignificant isomer
287 selectivity ($\text{IF}(Z) = 0.61 \pm 0.01$, $n = 10$). In contrast, $T_{1/2} = 19.6 \pm 3.2$ days for DIM in biotic

288 microcosms (Table 1) emphasised the prevailing contribution of DIM biodegradation to its
 289 overall dissipation in soil. Degradation of the (E)-isomer of DIM ($T_{1/2} \text{ (DIM-(E))} = 13.7 \pm 2.7$
 290 days) was faster than that of the (Z)-isomer ($T_{1/2} \text{ (DIM-(Z))} = 22.2 \pm 5.2$ days). These half-lives
 291 are in the range of those reported in previous field dissipation studies ($T_{1/2} \text{ (DIM-(Z))} = 9\text{-}86$ days
 292 and $T_{1/2} \text{ (DIM-(E))} = 11\text{-}30$ days) (FAO, 2014). Here, the vineyard soil used to derive $T_{1/2}$ was
 293 frequently treated with GripTop® (commercial formulation containing DIM), which may
 294 favour DIM-adapted microbial communities and higher DIM dissipation rates.

295 DIM-(Z) isomer fraction (IF(Z)) increased from 0.61 ± 0.01 up to 0.91 ± 0.01 ($n = 2$)
 296 after 100 days, indicating an enrichment in the DIM-(Z) isomer during biodegradation. The
 297 relationship between IF(Z) (or IR(Z)) and the degradation extent was significant ($r^2 > 0.97$, p^*
 298 < 0.001 , $n = 8$), yielding an IR enrichment factor ($\epsilon_{\text{IR}} = -54 \pm 6\%$) (Figure S6, equation 7).
 299 Although no ϵ_{IR} for DIM was previously retrieved, ϵ_{IR} for other organic molecules, including
 300 enantiomers, typically ranged from -4 to -237% (Esslinger et al., 2011; Jammer et al., 2015;
 301 Qiu et al., 2014; Souchier et al., 2016). Altogether, these results highlight significant isomer-
 302 selectivity during DIM biodegradation in soil.

303



304

305 *Figure 1: DIM concentrations (a) and IF(Z) (b) in biotic and abiotic soil experiments.*

306

307

3.2. Isomer-selective isotope analysis of DIM in soil microcosms

308 The carbon isotope composition ($\delta^{13}\text{C}$) of DIM in biotic soil experiments varied from
309 $\delta^{13}\text{C}_{\text{DIM-(Z)}} = -33.7 \pm 0.3 \text{ ‰}$ and $\delta^{13}\text{C}_{\text{DIM-(E)}} = -33.5 \pm 0.1 \text{ ‰}$ (t = 1 day) to $\delta^{13}\text{C}_{\text{DIM-(Z)}} = -29.1 \pm$
310 0.1 ‰ and $\delta^{13}\text{C}_{\text{DIM-(E)}} = -26.5 \pm 0.5 \text{ ‰}$ (t = 100 days). In contrast, no significant change of the
311 $\delta^{13}\text{C}$ of both DIM isomers after 100 days in the abiotic experiment confirmed no or limited
312 DIM biodegradation. Isotopic fractionation values for DIM-(Z) ($\epsilon_{\text{DIM-(Z)}} = -1.6 \pm 0.2 \text{ ‰}$,
313 equation 5) and DIM-(E) ($\epsilon_{\text{DIM-(E)}} = -1.5 \pm 0.2 \text{ ‰}$) in the biotic soil experiments were similar
314 (Table 1 and Figure S6). Since this is the first report for DIM bulk or isomer-selective isotopic
315 fractionation, ϵ_c values cannot be compared. The low isotopic fractionation values for DIM
316 reflect isotope dilution since the DIM molecule contains 21 carbon atoms. The two main
317 metabolites expected from a demethylation pathway are M550F006 (Z67, meta desmethyl
318 dimethomorph) and M550F007 (Z69, para desmethyl dimethomorph) (Avetta et al., 2014;
319 Zhang et al., 2020). However, the DIM degradation pathways in soil could not be confirmed
320 based on DIM degradation products as analytical standards are currently lacking.

321
322 *Table 1: DIM biodegradation kinetics and isomeric (ϵ_{IR}) and isotopic (ϵ_c) fractionation*
323 *observed in the laboratory biodegradation experiment with the vineyard soil.*

	$T_{1/2} \pm 95\% \text{ CI}$	$\epsilon_{\text{IR}} \pm 95\% \text{ CI}$	$\epsilon_c \pm 95\% \text{ CI}$
	[days]	[%]	[%]
DIM-(E)	13.7 ± 2.7		-1.6 ± 0.2
DIM-(Z)	22.2 ± 5.2	-54 ± 6	-1.5 ± 0.2
DIMtot	19.6 ± 3.2		-1.5 ± 0.2

324

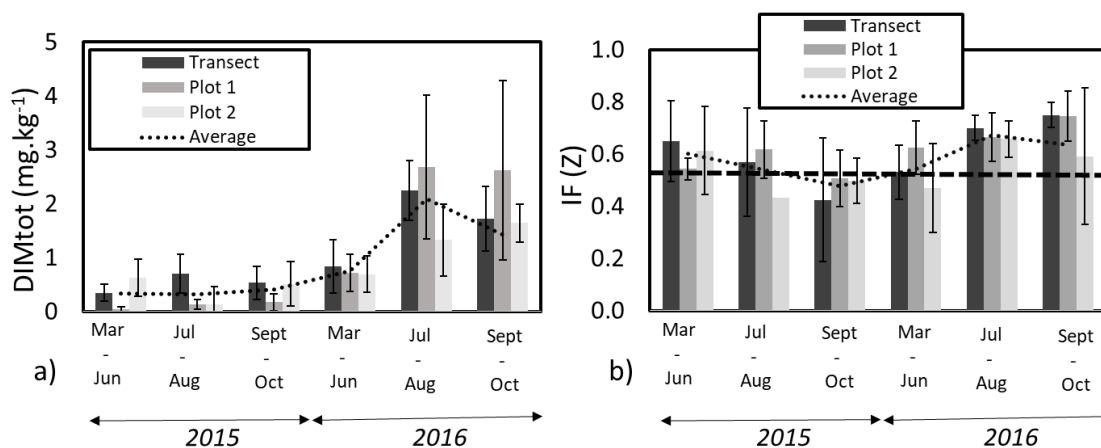
325 **3.3. DIM degradation and runoff transport in the vineyard plots**

326 Overall, the DIM concentrations in the soil significantly ($p < 0.001$) differed in 2015
327 ($0.25 \pm 0.12 \mu\text{g}\cdot\text{g}^{-1}$; n = 114, plots and catchment samples) and 2016 ($1.61 \pm 0.14 \mu\text{g}\cdot\text{g}^{-1}$; n =
328 93) and followed a seasonal application pattern. At the plot scale, DIM concentrations ranged

329 from below the DL up to $1.8 \mu\text{g}\cdot\text{g}^{-1}$ and $10.1 \mu\text{g}\cdot\text{g}^{-1}$ in the topsoil of the vineyard plots in 2015
 330 and 2016, respectively (Figure 2). The DIM concentrations in the P1 and P2 plots were
 331 similar ($p > 0.05$), confirming the reproducibility of the sampling strategy.

332 DIM_{tot} concentrations in runoff water from the plots ranged from $< \text{LD}$ up to $12 \mu\text{g}\cdot\text{L}^{-1}$
 333 and were above the French drinking water limit of $0.1 \mu\text{g}\cdot\text{L}^{-1}$ for 31 of the 39 samples.
 334 Although EFSA estimates that DIM acute toxicity towards aquatic organisms is low (EFSA,
 335 2006), several studies underscored an ecotoxic risk for several living organisms, including
 336 soil and water microflora (Avetta et al., 2014; Lunn, 2007) or in mixtures with other
 337 substances, such as difenoconazole (Fan et al., 2021) or copper (Megateli et al., 2013).

338 Altogether, isomeric fractionation values of the IF(Z) of DIM in the plot topsoil and
 339 runoff water indicated significant DIM degradation. Indeed, the IF(Z) values from 0.5 to 0.8
 340 in the vineyard plots in 2015 and 2016 were generally larger than the IF(Z) value of the DIM
 341 commercial formulation (GripTop®; 0.50 ± 0.02). This highlights that DIM-(Z) was
 342 systematically enriched in topsoil and runoff, while DIM-(E) degraded preferentially, in
 343 agreement with the results of the soil microcosm experiments. Similar IF(Z) values in topsoil
 344 and in runoff water at the plot scale suggest that DIM in runoff stems from a unique DIM pool
 345 in soil.



346

347 *Figure 2. DIM topsoil concentrations (a) and IF(Z) (b) at the plot and catchment scales. The*
 348 *periods correspond to vine budding and initial growth before DIM application (March–June),*
 349 *vine growth following DIM application (July–August) and the end of the season after*
 350 *harvesting (September–October). Dashed line in Figure 2b) represent the IF(Z) of the applied*
 351 *formulation.*

352 **3.4.DIM degradation and runoff transport in the vineyard catchment**

353 At the catchment scale, the DIM concentrations and IF(Z) in the topsoil were similar
 354 to those obtained at the plot scale (Figure 2), confirming the homogeneity of DIM
 355 applications. DIM concentrations in runoff collected at the catchment outlet were similar in
 356 2015 ($3.0 \pm 6.2 \mu\text{g. L}^{-1}$; n = 13) and 2016 ($5.0 \pm 9.5 \mu\text{g. L}^{-1}$; n = 15) (Table 2). The DIM mass
 357 export at the catchment outlet reached 2.3 g in 2015 and 4.7 g in 2016 (Imfeld et al., 2020).
 358 The DIM concentrations increased in both topsoil and runoff water following DIM
 359 application, with DIM export coefficients reaching 0.7% (Figure 3a and (Imfeld et al., 2020)).
 360 The DIM concentrations in topsoil in 2016 reached $2.9 \mu\text{g.g}^{-1}$ (June 22nd), during the main
 361 application (June 20th – 23th 2016), and gradually decreased to $1.2 \mu\text{g.g}^{-1}$ at the end of the
 362 sampling campaign (October 5th). Considering a layer of 1 cm of topsoil, this corresponds to
 363 DIM masses from 4.3 to 10 kg in the overall catchment topsoil. The DIM masses were similar
 364 to the applied masses (5.4 kg in 2016), supporting the idea of DIM storage in topsoil with
 365 limited yearly DIM degradation and export by surface runoff.

366 *Table 2: DIM concentrations, IF(Z) and $\delta^{13}\text{C}$ values in the vineyard catchment.*

Year	Rainfall depth (mm)	Outlet runoff volume (m ³)	Number of runoff events	Matrix	[DIM _{tot}] ($\mu\text{g.g}^{-1}$ or $\mu\text{g.L}^{-1}$)	IF(Z)	$\delta^{13}\text{C}_{\text{DIM-(Z)}}$ (‰)	$\delta^{13}\text{C}_{\text{DIM-(E)}}$ (‰)
					90 g.kg ⁻¹ *	0.50 ± 0.02 (n = 6)	-33.2 ± 0.7 (n = 3)	-33.7 ± 0.3 (n = 3)
2015	239	1577	32	Topsoil	0.11 ± 0.09 (n = 15)	0.63 ± 0.08 (n = 15)	n.d.	n.d.

				Runoff	3.0 ± 6.2 (n = 13)	0.81 ± 0.15 (n = 12)	-32.1 ± 0.9 (n = 7)	-29.2 ± 1.4 (n = 6)
2016	310	2027	47	Topsoil	1.5 ± 1.1 (n = 20)	0.65 ± 0.10 (n = 20)	-30.7 ± 1.7 (n = 8)	-28.6 ± 2.7 (n = 8)
				Runoff	5.0 ± 9.5 (n = 15)	0.72 ± 0.09 (n = 15)	n.d.	n.d.

367 *n.d.: not determined*

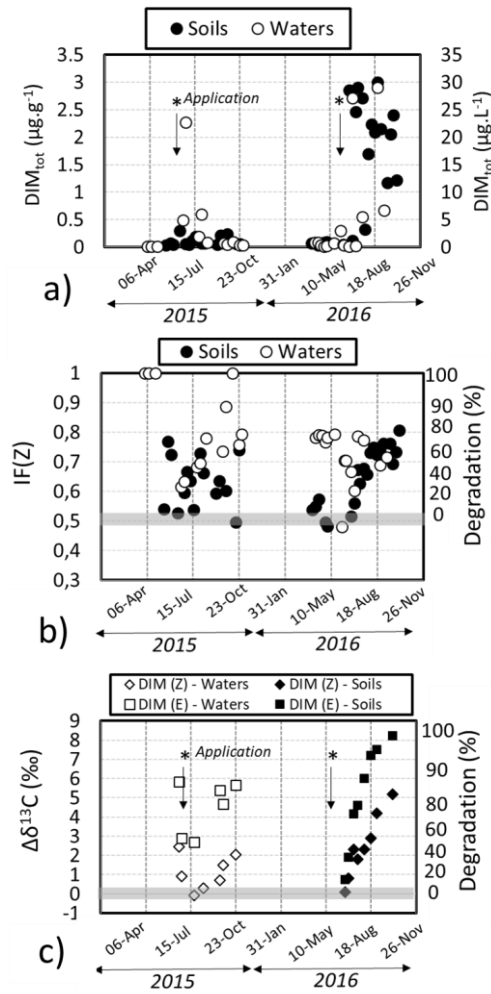
368 * DIM concentration in the commercial formulation Grip®Top (BASF)

369

370 The apparent DIM field dissipation of 128 ± 60 days ($T_{1/2 \text{ field}} \pm 95\% \text{ CI}$, n = 13) was
371 higher than the half-life of DIM ($T_{1/2 \text{ lab}} = 19.6 \pm 3.2 \text{ d}$) in laboratory experiments (Figure S7).
372 This indicates that DIM biodegradation was slower in the field than under laboratory-
373 controlled conditions. Overall, IF(Z) values reflected DIM applications, with IF(Z) in runoff
374 decreasing after DIM applications. IF(Z) >0.9 in runoff in early 2015 indicated degradation in
375 soil of the residual DIM from the previous DIM application in 2014. IF(Z) decreased to $\square 0.5$
376 following the application of the Griptop® formulation (IF(Z) = 0.50 ± 0.02 , Table 2), and
377 gradually increased up to 0.8-1 over time. In contrast, IF(Z) did not change much (IF(Z) =
378 0.63 ± 0.08) in topsoil across the 2015 season and was globally lower than in runoff water
379 (IF(Z) = 0.81 ± 0.15 Table 2).

380 IF(Z) variations in topsoil and runoff water were consistent with DIM biodegradation
381 estimates (Figure 3). IF(Z) in 2016 ranged from 0.6 to 0.8 in runoff, whereas it decreased after
382 DIM applications (June 20th to 23rd) and gradually increased from 0.5 to 0.8 in topsoil (Figure
383 3b). Accordingly, estimates of biodegradation extent (B(%)) derived from ϵ_{IR} values obtained
384 in laboratory experiments (equation 8) were significantly higher in the runoff water (B(%) =
385 $82 \pm 8\%$) than in the topsoil (B(%) = $58 \pm 10\%$) in 2015 and 2016 (Figure 3b). Overall, this
386 suggests a preferential export of the degraded fraction of DIM from the topsoil into the runoff
387 water. This supports the idea that DIM sorption ($K_{\text{oc}} = 300 - 600 \text{ L.kg}^{-1}$, (Boesten and
388 Matser, 2017)) may reduce the DIM bioavailability, and thus DIM degradation, in topsoil.

389
390
391
392



393

394 *Figure 3: Total DIM concentration (DIM_{tot}) (a), DIM isomeric fractionation ($IF(Z)$) (b), and DIM*
395 *isomer specific isotope composition for carbon ($\delta^{13}C$) compared to $\delta^{13}C$ of the commercial formulation*
396 *(c) in transect topsoils (filled symbols) and outlet runoff waters (empty symbols). DIM biodegradation*
397 *($B(\%)$) were estimated as described in the Materials and Methods section (equation 5 and 6).*

398
399

3.5. DIM isomer-specific isotopic fractionation in vineyard catchment topsoil and runoff

400 DIM ISIA was carried out in runoff (2015) and topsoil (2016) samples with sufficient
401 DIM concentrations (Figure 3c). In 2015, the initial $\delta^{13}\text{C}$ values of DIM in runoff ($\delta^{13}\text{C}_{\text{DIM-(Z)}}$
402 = $-30.7 \pm 1.2 \text{ ‰}$ and $\delta^{13}\text{C}_{\text{DIM-(E)}} = -27.9 \pm 1.2 \text{ ‰}$, June 18th) decreased ($\delta^{13}\text{C}_{\text{DIM-(Z)}} = -33.3 \pm$
403 1.9 ‰ $\delta^{13}\text{C}_{\text{DIM-(E)}} = -31.0 \pm 2.2 \text{ ‰}$, July 23rd) after DIM application, and were close to $\delta^{13}\text{C}_{\text{DIM}}$
404 value of the DIM commercial formulation (GripTop®; $\delta^{13}\text{C}_{\text{DIM-(Z)}} = -33.2 \pm 0.7$; $\delta^{13}\text{C}_{\text{DIM-(E)}} =$
405 -33.7 ± 0.3 , Table 2). However, the $\delta^{13}\text{C}$ values gradually increased ($\delta^{13}\text{C}_{\text{DIM-(Z)}} = -31.2 \pm 0.5$
406 ‰ ; $\delta^{13}\text{C}_{\text{DIM-(E)}} = -28.03 \pm 0.5 \text{ ‰}$) at the end of the season (Figure 3c). This gradual
407 enrichment in ^{13}C of the remaining DIM fraction exported during runoff indicates DIM
408 biodegradation in the vineyard soil, as previously observed with *S*-metolachlor in a crop
409 catchment (Alvarez-Zaldívar et al., 2018).

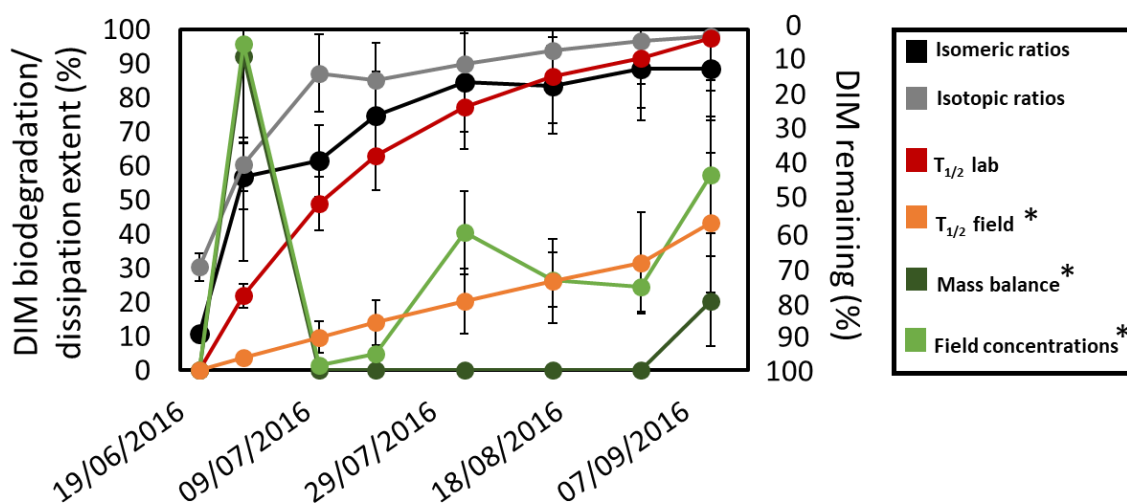
410 The isotopic fractionation values ($\epsilon_{\text{DIM-(Z)}} = -1.6 \pm 0.2 \text{ ‰}$ and $\epsilon_{\text{DIM-(E)}} = -1.5 \pm 0.2 \text{ ‰}$,
411 Table 1) derived from the soil microcosm experiments were used to estimate DIM
412 biodegradation, following the isotopic approach. Biodegradation estimates using the isotopic
413 approach (equation 6) ranged from 38 to 99% for DIM-(E) and from 0 to 97% for DIM-(Z) in
414 topsoil and runoff water (Figures 3c). Changes in DIM isotope signatures ($\Delta\delta^{13}\text{C}$ up to 6 ‰)
415 corresponded to an average biodegradation of 67% for DIM-(E) and 85% for DIM-(Z) in
416 topsoil, whereas biodegradation estimations in runoff average 44% for DIM-(E) and 92% for
417 DIM-(Z) (Figure 3c). Overall, DIM ISIA confirmed the gradual DIM degradation in topsoil
418 following DIM application.

419 ***3.6. Comparison of DIM degradation estimates in the vineyard catchment***

420 Overall, estimates of biodegradation extent B(%) obtained using the isomeric and
421 isotopic approaches in runoff significantly differed ($p < 0.05$), whereas B(%) in topsoil was
422 similar (Figure S8b). This suggests that distinct processes may affect DIM isomeric
423 fractionation in topsoil and runoff. For instance, DIM photolysis in water may lead to the fast
424 (i.e., a few minutes) interconversion of DIM isomers from (E) to (Z) (Avetta et al., 2014;

425 Lunn, 2007). In contrast, DIM sorbed in topsoil would be less prone to photolysis and
426 interconversion of DIM isomers. The interconversion during photolysis of DIM isomers in
427 runoff water may thus affect isomeric ratios since the water residence time in the vineyard
428 catchment ranges from 10 to 30 minutes. However, no isotope fractionation occurred ($\Delta\delta^{13}\text{C}$
429 $<1\text{‰}$ after 90% degradation, data not shown) during DIM photolysis in water under solar
430 irradiation (QSUN XE-1 test chamber, Xe arc lamp, and daylight-Q filter with a nominal cut-
431 on of 295 nm). Hence, DIM ISIA may lead to more accurate estimates of DIM biodegradation
432 than estimation relying on isomeric ratios since solar irradiation apparently has limited effect
433 on DIM $\delta^{13}\text{C}$ but may affect IF(Z) values.

434 Overall, estimates of B(%) or P(%) (proportion of remaining DIM) in topsoil at the
435 catchment scale largely differ depending on the estimation approach (Figure 4). The isotopic
436 and isomeric approaches yielded B(%) $>88\%$ in topsoil, which are close to B(%) estimates
437 obtained using laboratory half-life values ($T_{1/2} = 19.6\text{ d}$). B(%) estimated with isotopic,
438 isomeric and $T_{1/2}$ approaches from laboratory experiments were correlated ($R^2 > 0.86$, $p < 0.05$)
439 (Figure S9). However, estimates with these lab-derived approaches differed from the observed
440 $T_{1/2}$ (field) of 128 days derived from DIM concentrations in the vineyard soil after the DIM
441 application during the 2016 campaign (SI, Section S-5 and Figure S7). Similarly to $T_{1/2}$ (field)
442 approach, the so-called “field concentration” approach relies on comparing concentrations
443 shift in topsoils between t and t_0 (first samples after application date; SI, Section S-5).



444

445 *Figure 4: DIM dissipation in the vineyard soil following DIM application (2016) estimated*
 446 *with different approaches. See Section S-5 in the SI for calculations. *Estimation of*
 447 *dissipation extent (otherwise, biodegradation extent is estimated). Error bars represent the*
 448 *standard deviation of the method estimated via error propagation.*

449 This discrepancy between approaches suggests that the isotopic and isomeric
 450 approaches overestimated B(%) in the field and/or that using the field T_{1/2} value
 451 underestimated B(%). Estimates of DIM dissipation from DIM application onwards using the
 452 mass balance approach indicated that B(%) was close to zero (i.e., no DIM biodegradation) to
 453 balance DIM applications and stocks in the vineyard topsoil (SI, Section S-5). However, the
 454 mass balance results must be considered with caution because of the large uncertainties in
 455 such calculations. For instance, the low B(%) derived from this approach may be due to an
 456 overestimation of the DIM mass budget in soil (6920 ± 1594 g, 95% CI, n = 15, from June
 457 22nd to October 5th, 2016), which is based on the DIM concentrations in topsoil (i.e., top first
 458 cm) from transect. In addition, the doses of DIM application (5406 g in 2016, (Imfeld et al.,
 459 2020)) may have been underestimated when extrapolating the survey results to the entire
 460 catchment or due to underreporting of DIM usage by winegrowers.

461 Overall, the discrepancy among complementary approaches to estimate DIM
462 degradation highlights the interest and difficulties to quantify the contribution of pesticide
463 biodegradation to the overall dissipation in the field. Although different approaches yielded
464 similar estimates when examining S-metolachlor dissipation at the catchment scale (Alvarez-
465 Zaldívar et al., 2018), different approaches led to distinct estimates of DIM dissipation.
466 Several reasons may explain this difference. First, reference values derived from laboratory
467 experiments (i.e., isotopes, isomers and $T_{1/2}$ (lab)) may overestimate the dissipation compared
468 to field-derived parameters (i.e., mass balance, $T_{1/2}$ (field) and the field concentrations). This
469 may reflect the high sensitivity of DIM to degradation conditions, including microbial
470 communities, temperature, humidity, and DIM formulations, differing under laboratory and
471 field conditions. Second, additional degradation/volatilization and unknown processes
472 affecting DIM on the wine leaves may alter the isomeric and stable isotope composition of
473 DIM before it enters into the soil and runoff water. While S-metolachlor is applied directly to
474 soil, DIM is applied to leaves, where it is supposed to remain as long as possible to protect
475 plants from fungi after rainfall events. Indeed, the GripTop manufacturer (BASF) states that
476 DIM is safe from leaching once the spray has dried on the treated plant organs, approximately
477 one hour after treatment. Hence, DIM may persist (approximately 12-14 days) on the leaves
478 independent of the occurrence of rainfall. Overall, we hypothesise that the wine leaves may be
479 an important intermediate compartment before DIM reaches the soil. This also advocates
480 considering all compartments where pesticide degradation can occur once applied in the field
481 and carefully comparing field and laboratory degradation estimates.

482 **4. Conclusions**

483 Knowledge of the contribution of fungicide degradation to the overall dissipation in
484 agricultural catchments is scarce. In this study, we examined the potential of isomer and

485 stable isotope fractionation to evaluate DIM degradation at the vineyard plot and catchment
486 scales. Despite the large amount of carbon in the DIM molecule, significant carbon isotope
487 fractionation ($\Delta\delta^{13}\text{C} \approx 5 \text{ ‰}$) occurred during biodegradation in microcosm soil experiments
488 and in the field ($\Delta\delta^{13}\text{C}$ up to 7 ‰). Enrichment in both the (Z)-isomer and in ^{13}C of DIM
489 following DIM application indicated significant DIM degradation in both topsoil and runoff
490 water. Altogether, our results underscored substantial DIM immobilization in the vineyard
491 soil, while a small pool of bioavailable DIM may be degraded and exported by surface runoff
492 waters. Indeed, the isomeric approach, highlighted the preferential export of a highly
493 degraded fraction of DIM in runoff water compared to the DIM stored in the topsoil, with
494 limited (<1%) DIM export by surface runoff.

495 The comparison of the DIM degradation estimates obtained from isomeric and
496 isotopic fractionation with those retrieved from classical approaches, including $T_{1/2 \text{ (lab)}}$ and
497 $T_{1/2 \text{ (field)}}$, and mass balances, underlined the difficulty to use values derived from laboratory
498 experiments to estimate fungicide degradation in the field. For instance, the use of
499 degradation kinetics and values retrieved from the laboratory experiments (i.e., isotopic,
500 isomeric and $T_{1/2 \text{ (lab)}}$) overestimated the DIM dissipation compared to field estimates relying
501 on $T_{1/2 \text{ (field)}}$, mass balance, and field concentrations. Since fungicides are primarily applied to
502 plant leaves, the foliar compartment cannot be neglected as a potential site of degradation
503 processes, including photolysis and biodegradation, which may result in significant isomer
504 and/or isotope fractionation. Laboratory experiments targeting fungicide formulation
505 behaviour on leaf surfaces may help in the future to improve estimations of fungicide
506 degradation in vineyards. Overall, this study also emphasised the interest of crossing
507 independent information sources, including application surveys, and applying isotopic and
508 isomeric approaches to estimate fungicide degradation in agricultural catchments.

509

510 **Author contribution statement**

511 **Jérémy Masbou**: Conceptualization; Data curation; Formal analysis; Investigation;
512 Methodology; Visualization; Writing – original draft. **Sylvain Payraudeau**: Formal analysis;
513 Resources; Software; Validation; Writing – review & editing. **Benoit Guyot**: Data curation;
514 Formal analysis; Methodology; Writing – review & editing. **Gwenaël Imfeld**:
515 Conceptualization; Data curation; Formal analysis; Funding acquisition; Methodology;
516 Project administration; Resources; Supervision; Validation; Visualization; Writing – review &
517 editing.

518

519 **Declaration of competing interest**

520 The authors declare that they have no known competing financial interests or personal
521 relationships that could have appeared to influence the work reported in this paper.

522 **Data availability**

523 Data will be made available on request.

524 **Acknowledgements**

525 This research has been funded by the Agence de l'Eau Rhin-Meuse (AERM) and the Conseil
526 Interprofessionnel des Vins d'Alsace (CIVA) in the project PACOV and the French National
527 Research Agency ANR through grant ANR-18-CE04-0004-01, project DECISIVE. The
528 authors thank the Agricultural and Viticulture College of Rouffach (EPLEFPA Les Sillons de
529 Haute Alsace Rouffach), the City of Rouffach and the vine producers of the catchment. The

530 authors wish to acknowledge Eric Pernin and Agnès Herrmann for support in sampling,
531 analyses and surveys.

532 **Appendix A. Supplementary data**

533 Supplementary data to this article can be found online at

534 **References**

- 535 Alvarez-Zaldívar, P., Payraudeau, S., Meite, F., Masbou, J., Imfeld, G., 2018. Pesticide degradation and
536 export losses at the catchment scale: In sights from compound-specific isotope analysis
537 (CSIA). *Water Research*, 139: 198-207.
- 538 Avetta, P. et al., 2014. Phototransformation pathways of the fungicide dimethomorph ((E,Z) 4-[3-(4-
539 chlorophenyl)-3-(3,4-dimethoxyphenyl)-1-oxo-2-propenyl]morpholine), relevant to sunlit
540 surface waters. *Science of The Total Environment*, 500-501: 351-360.
- 541 Badea, S.-L., Danet, A.-F., 2015. Enantioselective stable isotope analysis (ESIA) — A new concept to
542 evaluate the environmental fate of chiral organic contaminants. *Science of The Total
543 Environment*, 514: 459-466.
- 544 Badea, S.L. et al., 2011. Development of an enantiomer-specific stable carbon isotope analysis (ESIA)
545 method for assessing the fate of α -hexachlorocyclo-hexane in the environment. *Rapid
546 Communications in Mass Spectrometry*, 25(10): 1363-1372.
- 547 Basheer, A.A., 2018. Chemical chiral pollution: impact on the society and science and need of the
548 regulations in the 21st century. *Chirality*, 30(4): 402-406.
- 549 Bashir, S., Fischer, A., Nijenhuis, I., Richnow, H.-H., 2013. Enantioselective carbon stable isotope
550 fractionation of hexachlorocyclohexane during aerobic biodegradation by *Sphingobium* spp.
551 *Environmental science & technology*, 47(20): 11432-11439.
- 552 Boesten, J., Matser, A., 2017. Sorption of pymetrozine and dimethomorph to substrate materials.
553 1566-7197, Wageningen Environmental Research.
- 554 Buser, H.-R., Poiger, T., Müller, M.D., 2000. Changed Enantiomer Composition of Metolachlor in
555 Surface Water Following the Introduction of the Enantiomerically Enriched Product to the
556 Market. *Environmental Science & Technology*, 34(13): 2690-2696.
- 557 Cui, G., Lartey-Young, G., Chen, C., Ma, L., 2021. Photodegradation of pesticides using compound-
558 specific isotope analysis (CSIA): a review. *RSC Advances*, 11(41): 25122-25140.
- 559 de Albuquerque, N.C.P., Carrão, D.B., Habenschus, M.D., de Oliveira, A.R.M., 2018. Metabolism
560 studies of chiral pesticides: A critical review. *Journal of pharmaceutical and biomedical
561 analysis*, 147: 89-109.
- 562 Drouin, G. et al., 2021. Direct and indirect photodegradation of atrazine and S-metolachlor in
563 agriculturally impacted surface water and associated C and N isotope fractionation.
564 *Environmental Science: Processes & Impacts*, 23(11): 1791-1802.
- 565 Droz, B. et al., 2021. Phase Transfer and Biodegradation of Pesticides in Water–Sediment Systems
566 Explored by Compound-Specific Isotope Analysis and Conceptual Modeling. *Environmental
567 Science & Technology*, 55(8): 4720-4728.
- 568 Duplay, J. et al., 2014. Copper, zinc, lead and cadmium bioavailability and retention in vineyard soils
569 (Rouffach, France): the impact of cultural practices. *Geoderma*, 230: 318-328.

570 EFSA, 2006. Conclusion regarding the peer review of the pesticide risk assessment of the active
571 substance dimethomorph. *EFSA Journal*, 4(7): 82r.

572 Elsner, M., McKelvie, J., Lacrampe Couloume, G., Sherwood Lollar, B., 2007. Insight into Methyl tert-
573 Butyl Ether (MTBE) Stable Isotope Fractionation from Abiotic Reference Experiments.
574 *Environmental Science & Technology*, 41(16): 5693-5700.

575 Esslinger, S., Becker, R., Maul, R., Nehls, I., 2011. Hexabromocyclododecane enantiomers:
576 microsomal degradation and patterns of hydroxylated metabolites. *Environmental science &
577 technology*, 45(9): 3938-3944.

578 Fan, R. et al., 2021. Combined Developmental Toxicity of the Pesticides Difenoconazole and
579 Dimethomorph on Embryonic Zebrafish. *Toxins*, 13(12): 854.

580 FAO, 2014. Dimetomorph Evaluation Report. 467-605.

581 Gámiz, B., Facenda, G., Celis, R., 2016. Evidence for the effect of sorption enantioselectivity on the
582 availability of chiral pesticide enantiomers in soil. *Environmental Pollution*, 213: 966-973.

583 Garrison, A.W., 2006. Probing the enantioselectivity of chiral pesticides. ACS Publications.

584 Gilevska, T. et al., 2022. Simple extraction methods for pesticide compound-specific isotope analysis
585 from environmental samples. *MethodsX*: 101880.

586 Hegeman, W.J., Laane, R., 2002. Enantiomeric enrichment of chiral pesticides in the environment.
587 *Reviews of environmental contamination and toxicology*, 173: 85-116.

588 Hengel, M.J., Shibamoto, T., 2000. Gas Chromatographic– Mass Spectrometric Method for the
589 Analysis of Dimethomorph Fungicide in Dried Hops. *Journal of agricultural and food
590 chemistry*, 48(12): 5824-5828.

591 Hoefs, J., 1997. Stable isotope geochemistry.

592 Höhener, P. et al., 2022. Multi-elemental compound-specific isotope analysis of pesticides for source
593 identification and monitoring of degradation in soil: a review. *Environmental Chemistry
594 Letters*: 1-16.

595 Huang, L., Lu, D., Diao, J., Zhou, Z., 2012. Enantioselective toxic effects and biodegradation of
596 benalaxyl in *Scenedesmus obliquus*. *Chemosphere*, 87(1): 7-11.

597 Hunkeler, D. et al., 2008. A guide for assessing biodegradation and source identification of organic
598 ground water contaminants using compound specific isotope analysis (CSIA). US EPA, Ada.

599 Imfeld, G. et al., 2020. Do rainfall characteristics affect the export of copper, zinc and synthetic
600 pesticides in surface runoff from headwater catchments? *Science of the Total Environment*,
601 741: 140437.

602 Jammer, S., Rizkov, D., Gelman, F., Lev, O., 2015. Quantitative structure–activity relationship
603 correlation between molecular structure and the Rayleigh enantiomeric enrichment factor.
604 *Environmental Science: Processes & Impacts*, 17(8): 1370-1376.

605 Jammer, S., Voloshenko, A., Gelman, F., Lev, O., 2014. Chiral and isotope analyses for assessing the
606 degradation of organic contaminants in the environment: Rayleigh dependence.
607 *Environmental science & technology*, 48(6): 3310-3318.

608 Jeschke, P., 2018. Current status of chirality in agrochemicals. *Pest management science*, 74(11):
609 2389-2404.

610 Jia, H.-f., Zhu, Y.-z., 2015. Screening and identification of spirodiclofen-degrading bacteria
611 *Enterobacter* sp. QD26-6 for soil under ginger cultivation. *Agrochemicals*, 54: 327-329.

612 Jin, B., Rolle, M., 2016. Joint interpretation of enantiomer and stable isotope fractionation for chiral
613 pesticides degradation. *Water research*, 105: 178-186.

614 Kurihara, N. et al., 1997. Pesticides report 37: Chirality in synthetic agrochemicals: Bioactivity and
615 safety consideration (Technical Report). *Pure and Applied Chemistry*, 69(9): 2007-2026.

616 Lefrancq, M. et al., 2014. Fungicides transport in runoff from vineyard plot and catchment:
617 contribution of non-target areas. *Environmental Science and Pollution Research*, 21(7): 4871-
618 4882.

619 Li, J. et al., 2013. Stereoisomeric Isolation and Stereoselective Fate of Insecticide Paichongding in
620 Flooded Paddy Soils. *Environmental Science & Technology*, 47(22): 12768-12774.

621 Li, X. et al., 2012. Enantioselective degradation of indoxacarb enantiomers in soils. *Environ. Chem*,
622 31: 1262-1267.

623 Liu, C., Wan, K., Huang, J., Wang, Y., Wang, F., 2012. Behavior of mixed formulation of metalaxyl and
624 dimethomorph in grape and soil under field conditions. *Ecotoxicology and environmental*
625 *safety*, 84: 112-116.

626 Liu, W., Gan, J., Schlenk, D., Jury, W.A., 2005. Enantioselectivity in environmental safety of current
627 chiral insecticides. *Proceedings of the National Academy of Sciences*, 102(3): 701-706.

628 Lunn, D., 2007. Dimethomorph. Food and Agriculture Organization of the United Nations.

629 Lutz, S.R. et al., 2017. Pesticide fate on catchment scale: conceptual modelling of stream CSIA data.
630 *Hydrology and Earth System Sciences*, 21(10): 5243.

631 Maier, M.P., Qiu, S., Elsner, M., 2013. Enantioselective stable isotope analysis (ESIA) of polar
632 herbicides. *Anal Bioanal Chem*, 405(9): 2825-31.

633 Masbou, J., Drouin, G., Payraudeau, S., Imfeld, G., 2018a. Carbon and nitrogen stable isotope
634 fractionation during abiotic hydrolysis of pesticides. *Chemosphere*, 213: 368-376.

635 Masbou, J., Meite, F., Guyot, B., Imfeld, G., 2018b. Enantiomer-specific stable carbon isotope analysis
636 (ESIA) to evaluate degradation of the chiral fungicide Metalaxyl in soils. *Journal of Hazardous*
637 *Materials*, 353: 99-107.

638 Megateli, S. et al., 2013. Simultaneous effects of two fungicides (copper and dimethomorph) on their
639 phytoremediation using *Lemna minor*. *Ecotoxicology*, 22(4): 683-692.

640 Melsbach, A. et al., 2020. Dual-element isotope analysis of desphenylchloridazon to investigate its
641 environmental fate in a systematic field study: a long-term lysimeter experiment.
642 *Environmental science & technology*, 54(7): 3929-3939.

643 Meyer, A.H., Penning, H., Elsner, M., 2009. C and N isotope fractionation suggests similar
644 mechanisms of microbial atrazine transformation despite involvement of different enzymes
645 (AtzA and TrzN). *Environmental science & technology*, 43(21): 8079-8085.

646 Milosevic, N. et al., 2013. Combined isotope and enantiomer analysis to assess the fate of phenoxy
647 acids in a heterogeneous geologic setting at an old landfill. *Water research*, 47(2): 637-649.

648 Pérez-Rodríguez, P., Schmitt, A.-D., Gangloff, S., Masbou, J., Imfeld, G., 2021. Plants affect the
649 dissipation and leaching of anilide pesticides in soil mesocosms: Insights from compound-
650 specific isotope analysis (CSIA). *Agriculture, Ecosystems & Environment*, 308: 107257.

651 Petrie, B., Barden, R., Kasprzyk-Hordern, B., 2015. A review on emerging contaminants in
652 wastewaters and the environment: current knowledge, understudied areas and
653 recommendations for future monitoring. *Water research*, 72: 3-27.

654 PPDBwebsite, Pesticides Properties DataBase - Dimethomorph.

655 Qiu, S. et al., 2014. Small $^{13}\text{C}/^{12}\text{C}$ Fractionation Contrasts with Large Enantiomer Fractionation in
656 Aerobic Biodegradation of Phenoxy Acids. *Environmental Science & Technology*, 48(10):
657 5501-5511.

658 Schürner, H.K. et al., 2016. Compound-Specific Stable Isotope Fractionation of Pesticides and
659 Pharmaceuticals in a Mesoscale Aquifer Model. *Environmental science & technology*.

660 Shabeer, A. et al., 2015. Residue dissipation and processing factor for dimethomorph, famoxadone
661 and cymoxanil during raisin preparation. *Food chemistry*, 170: 180-185.

662 Souchier, M., Benali-Raclot, D., Casellas, C., Ingrand, V., Chiron, S., 2016. Enantiomeric fractionation
663 as a tool for quantitative assessment of biodegradation: the case of metoprolol. *Water*
664 *research*, 95: 19-26.

665 Suryawanshi, K. et al., 2018. Field evaluation of the bio-efficacy of *Bacillus subtilis* DR-39 formulation
666 for enhancing pesticide degradation in grapes and optimisation of application dose. *Indian*
667 *Phytopathology*, 71(4): 571-577.

668 Tang, B., Luo, X.-J., Zeng, Y.-H., Mai, B.-X., 2017. Tracing the Biotransformation of PCBs and PBDEs in
669 Common Carp (*Cyprinus carpio*) Using Compound-Specific and Enantiomer-Specific Stable
670 Carbon Isotope Analysis. *Environmental Science & Technology*, 51(5): 2705-2713.

671 Torrentó, C. et al., 2021. Triple-element compound-specific stable isotope analysis (3D-CSIA): Added
672 value of Cl isotope ratios to assess herbicide degradation. *Environmental Science &*
673 *Technology*, 55(20): 13891-13901.

674 Tournebize, J., Gregoire, C., Coupe, R., Ackerer, P., 2012. Modelling nitrate transport under row
675 intercropping system: Vines and grass cover. *Journal of hydrology*, 440: 14-25.

676 Wang, J. et al., 2013. Compound-specific stable carbon isotope analysis of galaxolide enantiomers in
677 sediment using gas chromatography/isotope ratio monitoring mass spectrometry. *Rapid*
678 *Communications in Mass Spectrometry*, 27(15): 1690-1696.

679 Williams, G., Harrison, I., Carlick, C., Crowley, O., 2003. Changes in enantiomeric fraction as evidence
680 of natural attenuation of mecoprop in a limestone aquifer. *Journal of Contaminant*
681 *Hydrology*, 64(3-4): 253-267.

682 Wu, L. et al., 2018. Carbon and hydrogen isotope analysis of parathion for characterizing its natural
683 attenuation by hydrolysis at a contaminated site. *Water research*, 143: 146-154.

684 Xie, J. et al., 2018. Activity, toxicity, molecular docking, and environmental effects of three
685 imidazolinone herbicides enantiomers. *Science of the Total Environment*, 622: 594-602.

686 Yang, Z.-H., Ji, G.-D., 2015. Stereoselective Degradation and Molecular Ecological Mechanism of
687 Chiral Pesticides Beta-Cypermethrin in Soils with Different pH Values. *Environmental Science*
688 *& Technology*, 49(24): 14166-14175.

689 Zhai, W. et al., 2019. The biological activities of prothioconazole enantiomers and their toxicity
690 assessment on aquatic organisms. *Chirality*, 31(6): 468-475.

691 Zhang, C. et al., 2020. Rapid degradation of dimethomorph in polluted water and soil by *Bacillus*
692 *cereus* WL08 immobilized on bamboo charcoal–sodium alginate. *Journal of Hazardous*
693 *Materials*, 398: 122806.

694 Zhang, N. et al., 2014. Compound specific stable isotope analysis (CSIA) to characterize
695 transformation mechanisms of α -hexachlorocyclohexane. *Journal of hazardous materials*,
696 280: 750-757.

697